Hindawi
Advances in Meteorology
Volume 2019, Article ID 5250870, 14 pages
https://doi.org/10.1155/2019/5250870

Research Article

Impacts of Recent Climate Trends and Human Activity on the Land Cover Change of the Abbay River Basin in Ethiopia

Asaminew Abiyu Cherinet,[1] Denghua Yan,[1,2,3] Hao Wang,[1,2,3] Xinshan Song,[1] Tianlin Qin,[2,3] Mulualem T. Kassa,[4] Abel Girma,[1,5] Batsuren Dorjsuren,[6] Mohammed Gedefaw,[1,5] Hejia Wang,[7] and Otgonbayar Yadamjav[8]

[1]*College of Environmental Science and Engineering, Donghua University, Shanghai 201620, China*
[2]*State Key Laboratory of Simulation and Regulation of Water Cycle in River Basin, China Institute of Water Resources and Hydropower Research (IWHR), Beijing 100038, China*
[3]*Water Resources Department, China Institute of Water Resources and Hydropower Research (IWHR), Beijing 100038, China*
[4]*Bio-Taq Economy Innovations (BioTEI) Inc, Winnipeg, Canada*
[5]*Department of Natural Resource Management, University of Gondar, Gondar 196, Ethiopia*
[6]*Department of Environment and Forest Engineering, School of Engineering and Applied Sciences, National University of Mongolia, Ulaanbaatar 210646, Mongolia*
[7]*Department of Hydraulic Engineering, Tsinghua University, Haidian District, Beijing 100084, China*
[8]*Department of Sociology and Social Work, School of Art & Sciences, National University of Mongolia, Ulaanbaatar 210646, Mongolia*

Correspondence should be addressed to Denghua Yan; yandh@iwhr.com

Received 2 April 2019; Revised 9 August 2019; Accepted 5 September 2019; Published 15 October 2019

Guest Editor: Selahattin Incecik

The Abbay River Basin, which originates in Ethiopia, is a major tributary and main source of the Nile River Basin. Land cover and vegetation in the Abbay River Basin is highly susceptible to climate change. This study was conducted to investigate the trends of climate change for a period of thirty-six years (1980–2016) within selected stations of the basin by using the innovative trend analysis method, Mann–Kendall test, and Sen's slope estimator test to investigate the mean annual precipitation and temperature variables. Changes in land cover and vegetation in the Abbay River Basin were studied for a period of thirteen years (2001–2013) by using remote sensing, GIS analysis, land cover classification, and vegetation detection methods to assess the land cover and vegetation in the basin. In addition, Normalized Difference Vegetation Index (NDVI), Enhanced Vegetation Index (EVI), and Transformation Matrix were employed to analyze the spatial and temporal patterns of land cover and vegetation impacted by changes in climate. The result reflects that the trend of average annual temperature was remarkably increased ($\Phi = 0.12$, $Z = 0.75$) in the 36-year period, and the temperature was increased by 0.5°C, although precipitation had slightly decreased during the same period. In the thirteen years' period, forest land and water resource decreased by 3429.62 km^2 and 81.45 km^2, respectively. In contrast, an increment was observed in grassland (2779.33 km^2), cultivated land (535.34 km^2), bare land (43.08 km^2), urban land (0.65 km^2), and wetland (152.66 km^2) in the same period. In the study, it was also observed a decrease of an NDVI value by 0.1 was observed in 2013 in the southern part of the basin. The findings of the present study illustrate a significant change in eco-hydrological conditions in the ARB with an adverse impact on the environment. Hydroclimatic changes caused the increase in temperature and decreasing trend in precipitation which significantly impacted the land cover and vegetation in the basin. The changes in land cover were mostly caused by global and local climate influence which mainly affects the hydroclimate and eco-hydrology systems of the basin. The result is consistent with that of the previous studies conducted elsewhere. The findings of this paper could help researchers to understand the eco-hydrological condition of the study basin and become a foundation for further studies.

1. Introduction

Climate change is a major factor, which directly influences land cover and hydrology systems. In the past five decades, a global climatic change had been observed, leading to the changes in the hydrological cycle [1]. Climate change affects water resources by disrupting the hydrological system mainly through a change in quantity and quality of water, erratic water flow, timing, groundwater recharge, and others. Thus, future policies on water resources planning, development, and management should consider the impacts of climate change on land cover and water resources [2–4]. In addition, other forces of change such as demographic trends, climate variability, and national and macroeconomic policies alter the land cover which could, in turn, impact the hydrologic system [5]. Deforestation and plantation were the key factors of the land cover change. It is well-known that deforestation is a major cause of serious global environmental crisis [6]. As previously reported [6], deforestation of natural forests is a common phenomenon in the study basin. The land cover change could greatly alter the provision of ecosystem services. Vast areas of native grasslands, natural forests, and wetlands around the world had been destroyed and converted into croplands (for food production), tree plantations (for timber), and urban areas (housing). This alteration of the natural system had seriously impacted ecosystem services and biodiversity [5]. In developing countries, in particular, deforestation of forestlands had significantly been accelerated due to human needs for more agricultural lands for food production [7]. Another main cause of climate change is natural factors, which can bring either direct or indirect changes [8]. Land cover change, in general, is a key indicator of climate and human impacts on the environment. These include settlement and agricultural history, population growth and mobility, farming system practices, land and tree tenure systems, markets, and infrastructure and technological changes [9]. Land cover change is a very important topic in global change research. In the global scope, it plays an important role in the hydrothermal cycle of the global land water system [10]. As noted in the previous study [11], a land cover change had significant impacts on a global environmental change that affects the quantity of water in the ecosystems.

The Abbay River Basin has a dynamic change in land cover exacerbated by a high rate of population growth and climate change in the region. There is evidence that had shown forest lands being replaced by food crops [12]. Croplands usage is primarily shifted to coffee or Eucalyptus tree plantation [12]. Recent reports had also shown a significant increase in urbanization in the region with a higher rate (16%) of urban population growth [13, 14]. The high demands for fuelwood and construction materials have significantly enhanced the plantation of Eucalyptus trees in the region [15]. These shifts in land cover profile had cascading effects on ecosystem services and pose serious challenges in the region [16]. In this study, we analyzed the overall trends and changes of the land cover on ecosystem services using a transformation matrix for a period of 13 years (2001–2013) and historical climate change trends for 36 years (1980–2016). The study had also analyzed vegetation evolution assessment to identify the level of change in vegetation cover using Normalized Difference Vegetation Index (NDVI) and Enhanced Vegetation Index (EVI).

2. Materials and Methods

2.1. Study Area. Abbay River Basin is located in the northwestern region of Ethiopia between 7°40′N and 12°51′N latitude and 34°25′E and 39°49′E longitude. It covers an area of 199,592.17 km^2 [17] and extends to Amhara, Oromia, and Benishan-gul-Gumuz regional states. It shares a boundary with the Tekeze Basin to the north, the Awash Basin to the east and southeast, the Omo-Gibe Basin to the south, and the Baro-Akobo Basin to the southwest. The country's largest freshwater lake, Lake Tana, is the source of the Abbay River Basin and is located north of the basin. The basin is subdivided into 16 subbasins based on major rivers in the basin and its tributaries [13, 17, 18]. The Abbay River Basin is a land of dramatic gorges and mountains and is the most important river basin in Ethiopia. It is the major source of water for the Nile River Basin (Figure 1).

2.2. Data Sources

2.2.1. Land Cover Data Sources. The land cover satellite data of the study area were collected from the Ministry of Energy and Water Resources of Ethiopia. The data were found from Global Land Covers Dataset (GlobeLand30) as described by the National Geometrics Center of China in 2014 (Table 1). It shows the name, code, and definition of land cover classification and Landsat Thematic Mapper (TM) and Enhanced Thematic Mapper Plus (ETM+) data with a resolution of 30 m for thirteen-year period (2001 to 2013). Images data files were downloaded from the United State Geological Survey (USGS) website and extracted to Tiff format files to interpret the land cover spatial pattern data for the 13-year (2001–2013) period. In this study, the expanded classification system was adopted to sufficiently capture the local characteristics of the study area (Table 1). To understand the overall changes in land cover, matrix changes were analyzed and mapped [16]. Prior to classification, pre-image-processing operations including image restoration, georeferencing, and image enhancement were performed. Ecological landscape potential map, topographic, forest, and vegetation maps were chosen for accuracy testing and validation. The accuracy was tested after classification with accuracy assessment tools using representative data points.

2.2.2. Meteorology Data Sources. As cited in a previous study [19], the baseline climate scenario represents current climate conditions, particularly precipitation and temperature patterns. As in most climate change studies, this study uses average annual precipitation and temperature data from thirty-six years (1980 to 2016). Data for current climate conditions of the study area were acquired from the Ministry of Energy and Water Resources of Ethiopia, the National Meteorological Agency of Ethiopia. The data were collected from 5 different stations from four regional states and were derived from the National Oceanic and Atmospheric

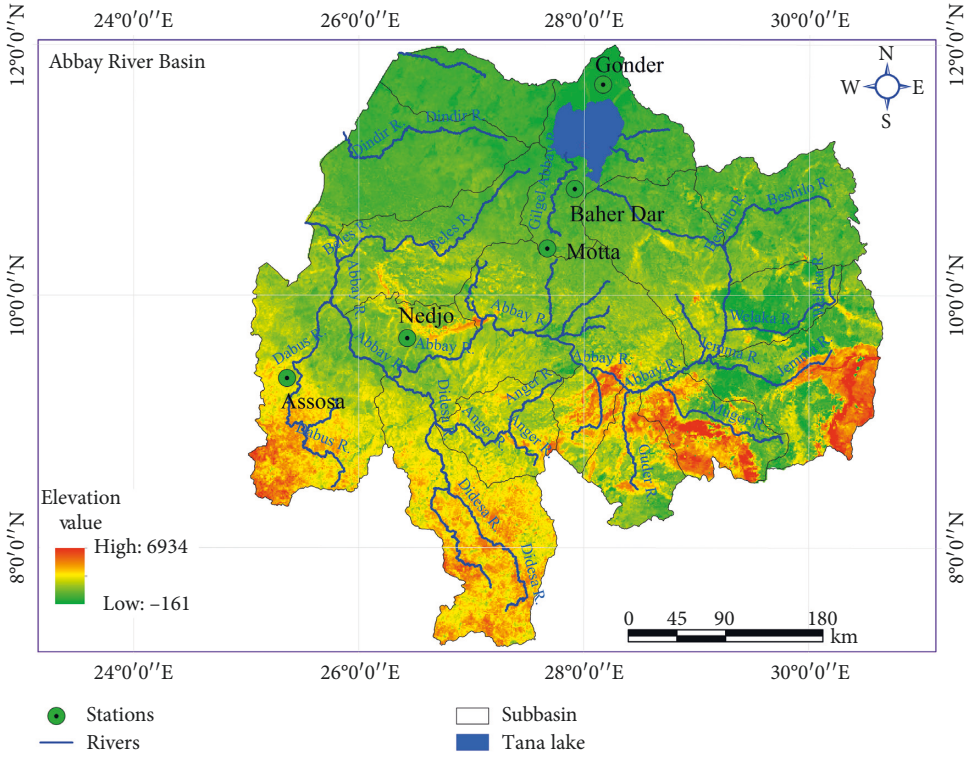

Figure 1: Digital elevation map (DEM) of Ethiopia and location map of the study area.

Table 1: Land covers types and their detail descriptions in Abbay River Basin.

Land cover types	Code	Description
Bare land	Bl	Areas of land that are poorly covered by vegetation due to erosion, overgrazing, cultivation, mining area, etc.
Cultivated land	Cl	Lands used for agriculture, horticulture, and gardens, including paddy fields, irrigated and dry farmland, vegetation and fruit gardens, etc.
Forest land	Fl	Lands covered with trees, with vegetation cover over 30%, including deciduous and coniferous forests, and sparse woodland with cover 10–30%, etc.
Grass land	Gl	Lands covered by natural grass with cover over 10%, etc.
Urban	Ur	Lands modified by human activities, including all kinds of habitation, residential, commercial, industrial, transportation facilities, interior urban green zones, etc.
Water	Wa	Water bodies in the land area, including river, lake, reservoir, fish pond, lands covered by temporally snow, glacier and icecap, etc.
Wetland	Wl	Lands covered with wetland plants and water bodies, including inland marsh, lake marsh, river floodplain wetland, forest/shrub wetland, peat bogs, mangrove and salt marsh, etc.

Administration (NOAA), National Centers for Environmental Information (NCEI).

2.2.3. Vegetation Data Sources. Normalized Difference Vegetation Index (NDVI) and Enhanced Vegetation Index (EVI) data were extracted by referencing the Moderate Resolution Imaging Spectra Radiometer Enhanced Vegetation Index (MODIS NDVI) product (MOD13Q1) obtained from NASA. The NDVI was calculated from the MODIS land-surface reflectance values from the red band (610–680 nm) and near-infrared band (780–890 nm) and corrected with molecular scattering, ozone absorption, and aerosols [9]. The MOD13A3 products, which include 12

scientific data sets with a 250 m by 250 m spatial resolution and a 16-day temporal sampling period, were derived from the latest version (Collection 6) from 1st September to 16th September in both 2001 and 2013. The MOD13Q1 products were downloaded from USGS (https://lpdaac.usgs.gov/).

2.3. Methods

2.3.1. Land Cover Analysis. Classified and unclassified maps of the study area were generated based on a classification scheme with a maximum likelihood classifier (Table 1). Abbay River Basin landscape was classified into seven land classes (Figure 2). Land cover maps of the study area for the year 2001 and 2013 were generated from Landsat TM and ETM+ imagery classification. Land cover change extent was determined as previously described [20]. The analysis evaluates the changes in land cover over time to establish the relationship between land cover changes and spatial patterns using overlapping operation. The analysis was conducted using postclassification comparison method where Landsat image for each year was classified and labeled independently followed by a comparison using an overlay procedure [21]. The magnitudes of change in terms of land cover were determined using the method described by [22]. The variables were calculated as follows:

$$A = \mathrm{TA}(t_2) - \mathrm{TA}(t_1), \tag{1}$$

$$\mathrm{CE} = \left[\frac{\mathrm{CA}}{\mathrm{TA}(t_1)}\right] * 100, \tag{2}$$

where TA is the total area, CA is the changed area, CE is the change extent, and t_1 and t_2 are the beginning and ending times the land cover studies were conducted.

It is worth noting here that the widest classification accuracy used by most researchers is in the form of an error matrix, which is used to derive a series of descriptive and analytical statistics. As described in [21, 23], assessment of classification accuracy for 2001 and 2013 images was conducted to determine the quality of information derived from the data. It was coupled with previous knowledge of the area and used as reference data. If classification data are to be useful in detecting change analysis, it is important to perform an accuracy assessment for each individual classification. Kappa coefficient and error matrix are standard measures of the reliability and accuracy of the maps produced. The Kappa statistics were determined in this study while the methods were described in detail in the previous studies [24, 25]. Kappa coefficient was calculated using the following equations [21]:

$$K = \frac{P(A) - P(E)}{1 - P(E)}, \tag{3}$$

$$P(A) = \frac{(A + D)}{N}, \tag{4}$$

$$(E) = \left(\frac{A1}{N}\right) * \left(\frac{B1}{N}\right) + \left(\frac{A2}{N}\right) * \left(\frac{B2}{N}\right), \tag{5}$$

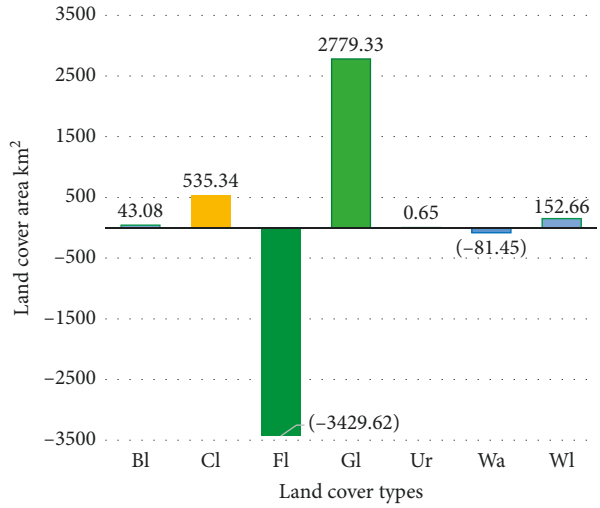

Figure 2: Land cover change extent in 2001 and 2013 of the study area.

where K is the Kappa coefficient, $P(A)$ is the number of times the k raters agree, and $P(E)$ is the number of times the k raters are expected to agree only by chance [26], A and D are the unchanged categories, $A1$ and $B1$ are the subject's categories, and N is the change of results.

2.3.2. Vegetation Analysis. Normalized Difference Vegetation Index (NDVI) metric and the coarse spatial resolution were primarily used for testing possible methodologies and were supported by ground-based information [9]. Vegetation attributes were used in various models to study photosynthesis, carbon budget, water balance, and related terrestrial processes [27]. The MODIS Vegetation Index was developed within 16 days of variation, and at multiple spatial resolutions to provide consistent spatial and modern comparisons of leafy surroundings, a composite property of leaf area, chlorophyll and canopy structures. The common compositing time of 8–14 days provides at least 25–30 global NDVI datasets per year as described in [28]. These products characterize more effectively the global range of vegetation states and processes. The MODIS Normalized Difference Vegetation Index (NDVI) complements NOAA's Advanced Very-High-Resolution Radiometer (AVHRR) NDVI products and provides continuity for time series historical applications. Enhanced Vegetation Index (EVI), which minimizes canopy soil variation, was used to improve sensitivity over dense vegetation conditions. Vegetation cover was determined using the NDVI and EVI matrices (Figure 2). Normalized Difference Vegetation Index (NDVI) is the most widely used vegetation index to distinguish between healthy vegetation from others (e.g., nonvegetated areas) [25]. NDVI is one of the indicators for the vegetative greenness of an area, and therefore, changes in NDVI are changes in vegetation and vegetation indices, which is an indirect indicator of plant biomass and vegetation activity [27, 29]. It is derived using the following expression:

$$\text{NDVI} = \frac{(\text{NIR} - \text{RED})}{(\text{NIR} + \text{RED})}, \quad (6)$$

where NIR is the near-infrared and RED is the red channel of the electromagnetic spectrum, corresponding to bands 2 and 1 of the MODIS (MOD13Q1) product.

The study also explored the conceptual and methodological issues that arise when scaling the use of NDVI for obtaining information on land cover from country to the study area scale. The second vegetation layer is the Enhanced Vegetation Index (EVI), which has improved sensitivity for high biomass regions and was calculated using the following equation:

$$D = \frac{(\text{NDVI} - \text{NDVI}_{\text{min}})}{(\text{NDVI}_{\text{max}} - \text{NDVI}_{\text{min}})}, \quad (7)$$

where NDVI_{max} and NDVI_{min} represent the maximum and minimum NDVI values for each vegetation (forest, grassland, shrub land) class. Afterwards, the values of the cover density index were classified into four ranges (<20, 20–50, 50–80, and >80%). Integration, spatial analysis, and any calculations were carried out in the GIS environment (QGIS 1.8, GRASS 6.4.2). The geographic information was projected to WGS84 UTM zone 33.

2.3.3. Meteorology Analysis. Metrological data like average annual Temperature and precipitation data from 5 stations were investigated in the Abbay River Basin from different representative stations of the study area (Table 2). Based on the class of the stations, the number of climate variables collected varies from stations to stations. Observe the selected climate stations in the Abbay River Basin are taken into indicator in the following table classification class's considerations. Climate data were calculated on 5 metrological stations of Assosa, Bahir Dar, Gondar, Nedjo, and Motta for analytical mathematics method.

(1) Innovative Trend Analysis Method (ITAM). The innovative trend analysis method (ITAM) divides a time series into two equal parts, and it sorts both subseries in the ascending order [6, 30–34]. Then, the two halves are placed on a coordinate system $(x_i : i = 1, 2, 3, \ldots, n/2)$ on X-axis and $(x_j : j = n/2 + 1, n/2 + 2, \ldots, n)$ on Y-axis. If the time series data on a scattered plot are collected on the 1 : 1 (45°) straight line, it indicates no trend. However, the trend is increasing when data points accumulate above the 1 : 1 straight line and the trend is decreasing when data points accumulate below the 1 : 1 straight line. The mean value difference between x_i and x_j could give the trend magnitude of data series. The first observed data point was not considered in this study when classifying the time series data into x_i and x_j data points have a different size (Figure 3).

Annual precipitation is 36 years from 1980–2016, and annual temperature is 36 years from 1980 to 2016. The direction of the trend is also affected by x_i data series. The trend indicator of ITAM is multiplied by 10 to make the scale similar to the other two tests. The trend indicator is given as follows:

Table 2: Names of meteorology stations, longitude, latitude, and elevation of the study area.

No.	Name of stations	Longitude E	Latitude N	Elevation (m)
1	Bahir Dar	37°22′59.99″E	11°35′59.99″N	1770
2	Gondar	37°27′59.99″E	12°35′59.99″N	1967
3	Motta	37°51′59.99″E	11°04′60.00″N	2440
4	Assosa	34°30′59.99″E	10°03′60.00″N	1600
5	Nedjo	35°29′59.99″E	9°29′59.99″N	1800

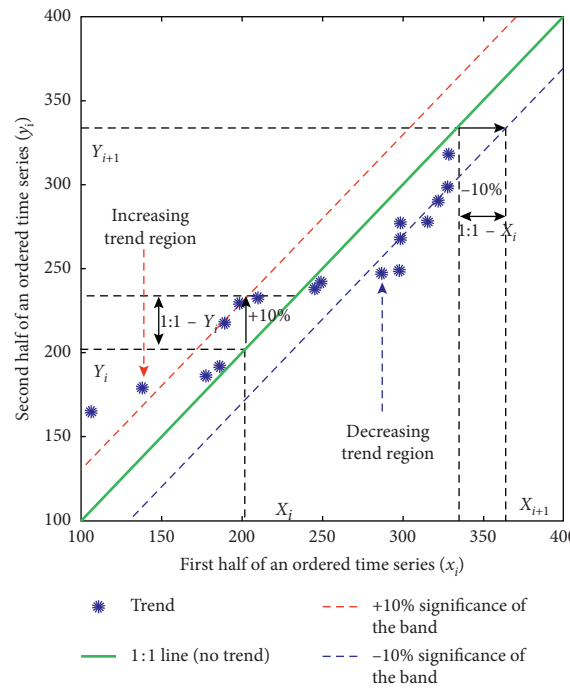

Figure 3: Paradigmatic of the ITA method.

$$\Phi = \frac{1}{n}\sum_{i=1}^{n}\frac{10\left(x_j - x_i\right)}{\mu}, \quad (8)$$

where Φ = trend indicator, n = number of observation on the subseries, x_i = data series in the first half subseries class, x_j = data series in the second half subseries part, and μ = mean of data series in the first half subseries part. A positive value of Φ indicates an increasing trend. However, a negative value of Φ indicates a decreasing trend. However, when the scatter points are closest around the 1 : 1 straight line, it implies the nonexistence of a significant trend.

(2) Mann–Kendall Trend Test. The Mann–Kendall (MK) trend test is a nonparametric test commonly employed to detect changing trends in a series of environmental data, climate data, or hydrological data [28, 31, 35–37]. The Mann–Kendall (MK) test method also shows upward and downward trends with statistical significance. The strength of the trend depends on the magnitude, sample size, and variations of data series. When the data point of later year is larger than the data point of the previous year, the MK statistics is increased by one otherwise the MK statistics

decreased by one. Thus, the MK statistics is the cumulative result of all the data values. The Mann–Kendall test statistics "S" is then equated as follows:

$$S = \sum_{i=1}^{n-1} \sum_{j=i+1}^{n} \operatorname{sgn}\left(x_j - x_i\right). \tag{9}$$

The trend test is applied to x_i data values $(i = 1, 2, \ldots, n-1)$ and x_j $(j = i+1, 2, \ldots, n)$. The data value of each x_i is used as a reference point to compare with the data value of x_j which is given as follows:

$$\operatorname{sgn}\left(x_j - x_i\right) = \begin{cases} +1, \text{if}\left(x_j - x_i\right) > 0, \\ 0, \text{ if}\left(x_j - x_i\right) = 0, \\ -1, \text{if}\left(x_j - x_i\right) < 0, \end{cases} \tag{10}$$

where x_j and x_i are the values in periods j and i. When the number of data series greater than or equal to ten $(n \geq 10)$, the MK test is then characterized by a normal distribution with the mean $E(S) = 0$ and variance $\operatorname{Var}(S)$ is equated as follows:

$$E(S) = 0, \tag{11}$$

$$\operatorname{Var}(S) = \frac{n(n-1)(2n+5) - \sum_{k=1}^{m} t_k \left(t_k - 1\right)\left(2t_k + 5\right)}{18}, \tag{12}$$

where m is the number of the tied groups in the time series and t_k is the number of ties in the kth tied group. The test statistics Z is as follows:

$$Z = \begin{cases} \dfrac{s-1}{\delta}, & \text{if } S > 0, \\ 0, & \text{if } S = 0, \\ \dfrac{s+1}{\delta}, & \text{if } S < 0. \end{cases} \tag{13}$$

When Z is greater than zero, it indicates an increasing trend and when Z is less than zero, it is a decreasing trend.

(3) Sen's Slope Estimator Test. Sen's Slope Estimator has been used extensively in meteorological time series and equally applicable where data gap exists [38]. The trend magnitude is calculated by slope estimator methods. The slope Q_i between two data points is given by the following equation:

$$Q_i = \frac{x_j - x_k}{j - k}, \quad \text{for } i = 1, 2, \ldots, N, \tag{14}$$

where x_j and x_k are data points at time j and $(j > k)$, respectively. When there is only single datum in each time, then $N = n(n-1)/2$; n is the number of time periods. However, if the number of data in each year is high, then $N < n(n-1)/2$; n is the total number of observations [39]. The N values of slope estimator are arranged from smallest to biggest. Then, the median of slope (β) is computed as follows:

$$\beta = \begin{cases} Q\left[\dfrac{N+1}{2}\right], & \text{when } N \text{ is odd}, \\ Q\left[\dfrac{(N/2) + Q(N+2)/2}{2}\right], & \text{when } N \text{ is even}. \end{cases} \tag{15}$$

The sign of β shows whether the trend is increasing or decreasing. When Q_i is positive, it means that there is an increasing or upward trend, while the negative value of Q_i reveals decreasing or downward trend in time series analysis. Similarly, zero value indicates no trend.

3. Results and Discussion

3.1. Classification of Land Cover Type and Change Detection. The results show a degree of land cover changes over a period of 13 years (2001–2013). During this period (2001–2013), grassland was the dominant vegetation type followed by cultivated land and bare land (Table 3; Figures 2 and 4). In the same period, it was observed that the forest land and water bodies were reduced (Table 3; Figures 2 and 4). The result in this study is consistent with that of the previous reports [6] and found that forest land cover was significantly diminished particularly in the northern part of the study region. The seven land cover classes identified in the study area were cultivated land, forest land, grassland, water body, wetland, bare land, and urban land (Figures 2 and 4; Table 3). The number of classified pixels increased for cultivated land (Cl), grassland (Gl), and wetland (We) but decreased for of forest land (Fl) and water body (Wl) (Figure 2). During the 13-year period, significant changes in the study area occurred particularly in forest land and water bodies, respectively, and the former decreased by 3429.62 km^2 (1.72%) while the latter decreased by 81.45 km^2 (0.04%), respectively. On the contrary, cultivated land, grassland, wetland, bare land, and urban land were increased by 535.34 km^2 (0.27%), 2779.33 km^2 (1.39%), 152.66 km^2 (0.08%), 43.08 km^2 (0.02%), and 0.65 km^2 (0.0003%), respectively (Table 3 and Figure 4). Cultivated land, grassland, wetland, bare land, and urban covers were slightly increased in area at the end of the study period compared to that of at the beginning of the study period. However, there were both increments and reductions in these land classes between the different observation points (Figure 4) and SAT.

Human activities associated with economic factors are commonly cited as a major stimulus for land cover change [24]. The increasing trend of land cover change observed in this study is associated mainly with economic forces. It was observed in the study that forest covers were mostly surrounded by farmlands, particularly in the catchment area and the increase in population density in the area clear forest lands to provide farmlands for food production [6].

Total forest cover in the study area reduced by half between 1957 and 2000 [6, 8]. In general, the result reported in this study is similar in accuracy of change of the listed previous studies (Figure 2).

As reported in the previous studies [23, 24, 26], the accuracy of individual classifications is very important to generate useful data for the land cover change study. There

Table 3: Changing present of land covers in 2001 and 2013.

No.	Land cover types	Initial area 2001		Final area 2013		Changing status	
		km^2	%	km^2	%	km^2	%
1	Bare land	12.28	0.01	55.36	0.03	43.08	0.02
2	Cultivated land	58249.08	29.18	58784.42	29.45	535.34	0.27
3	Forest land	6460.33	3.24	3030.72	1.52	(−3429.62)	−1.72
4	Grass land	131551.69	65.91	134331.01	67.30	2779.33	1.39
5	Urban	89.45	0.04	90.10	0.05	0.65	0.0003
6	Water	3141.27	1.57	3059.82	1.53	(−81.45)	−0.04
7	Wetland	88.08	0.04	240.74	0.12	152.66	0.08

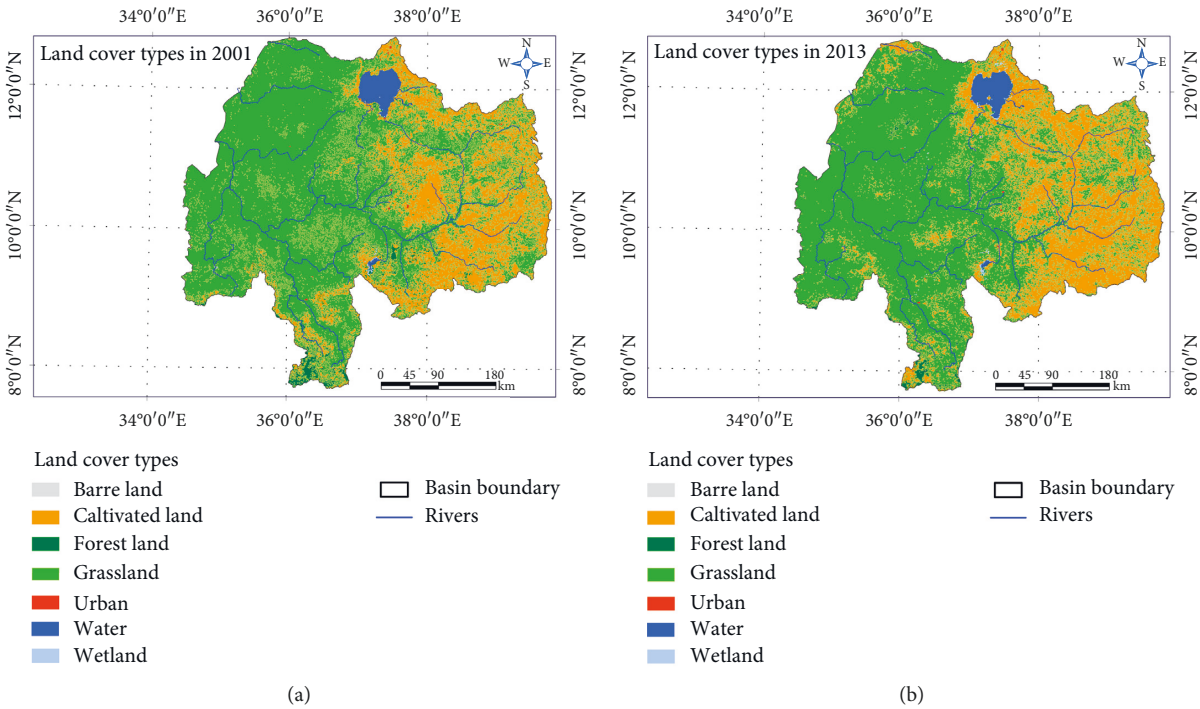

Figure 4: Classification of the changing land cover map of Abbay River Basin (2001 and 2013) Derived from Landsat TM/ETM+ images: (a) description of land cover in 2001 and (b) description of land cover and change in 2013.

are various ways of conducting change detection analysis. In this study, a land cover classification for the year 2001 and 2013 was produced, and the accuracy assessments were checked using 0.89 Kappa coefficient of the transformation matrix (Table 4). The statistical Kappa coefficient classification accuracy recommended value ranges from 0.18 to 0.99. Thus, the result in this study is considered almost in perfect agreement based on the Kappa Statistics. This implies that the change detection results could be used for further analysis as land cover transformation matrix and ArcGIS 10.4 were employed to analyze a comprehensive land use dynamics degree [40].

Following anthropogenic effects, climate change is the most important driving force that impacts land cover change and water resources. This study revealed the dynamic of changes in land cover particularly forest land and indirectly the impacts on the water resources system of the basin. As reported in [41], the catchment in the study area was converted to farmlands and human settlements from other land use (e.g., forest land) in various years. The land cover map of 2001–2013 in Table 4 shows that forest land cover of about 555.01 km^2 was converted into cultivated land, 2965.44 km^2 into grassland, 42.83 km^2 into the wetland, and 2.67 km^2 into bare land. Of the coverage of water resources, 50.43 km^2 was changed into wetland, 21.30 km^2 converted to bare land, 11.75 km^2 into forest land, and 5.05 km^2 converted to grassland. In general, during the 13-year period (2001–2013), cultivated land had increased by 535.34 km^2, the increase of grassland (2779.33 km^2), wetland (+152.66 km^2), bare land (+43.08 km^2), and urban (+0.65 km^2). However, forest land and water bodies were decreased by 3429.62 km^2 (1.72%) and 81.45 km^2 (0.04%), respectively. The individual class areas and change statistics for the two periods are summarized in Tables 3 and 4. The change indicates that there is a driving force that impacted a visible land cover change. Several researchers had warned the serious impacts of climate change and human activities on water resources and the ecosystem of the basin [14, 41, 42], and the results of this study are consistent with the findings of these studies.

Table 4: Comparison of the process change of land covers in 2001 and 2013.

		Land cover types (2001)							
	Types	Bl	Cl	Fl	Gl	Ur	Wa	Wl	Total
Land cover types (2013)	Bl	7.61	3.69	2.67	18.09	0.00	21.30	2.00	**55.36**
	Cl	0.00	55179.84	555.01	3041.43	4.37	0.07	3.72	**58784.42**
	Fl	0.00	74.02	2893.03	36.67	0.00	11.75	15.25	**3030.72**
	Gl	1.00	2953.95	2965.44	128386.35	2.08	5.05	17.15	**134331.01**
	Ur	0.00	3.68	0.03	4.38	82.00	0.00	0.00	**90.10**
	Wa	1.03	2.68	1.33	0.92	0.00	3052.68	1.18	**3059.82**
	Wl	2.64	31.22	42.83	63.84	1.00	50.43	48.78	**240.74**
	Total	**12.28**	**58249.08**	**6460.33**	**131551.69**	**89.45**	**3141.27**	**88.08**	

3.2. Measuring Vegetation (NDVI and EVI). Common values of the pixel varied between −1 and 1. The highest values of NDVI were >0.3, indicating rich or healthy vegetation. In this study, conversation of forest and grasslands into agricultural land was found to be the main cause of land cover change. The change had affected the hydro-ecological system of the region particularly due to the high requirement of irrigation water to support crop production. The maximum value of NDVI ranges from 0.99 to −0.19 in 2001, and the minimum value ranges from 0.99 to −0.20 in 2013. Significant land cover change occurs in the southern part of the studied area, while on the other sides, insignificant vegetation cover change was observed Figure 5. A vegetation cover is an important factor that could change the ecosystem and the hydrology pattern in the basin, thereby causing climate variability. Vegetation dynamics could change the global carbon and hydrology cycle as well as climate change [40]. The overlaps of the NDVI, EVI maps of 2001 and 2013, and climatic variations of the current weather show a high degree of climate change occurring across the basin.

3.3. Climate Trends in the Basin. In recent years, attention had been given to look the potential effects of climate change on the basin. In fact, some studies had shown that the water resources are critically sensitive to climate change [2, 3]. In a 36-year period (1980–2016), the temperature in the basin was increased by 0.5°C or 0.14°C per year. The minimum and the maximum recorded temperatures were 19.25°C and 17.00°C per year, respectively. In the study region, the observed temperature was increased from 1980 to 2016 ($y = 0.0039x + 19.349$) (Figure 6).

The global mean temperature had risen by about 0.85 from 1880 to 2012 and is expected to grow steadily. Global warming can change the region hydrology and inflows river ecosystem quickly. The temperature inland water bodies around the world had been rapidly warming since 1985 with an average rate between 0.045 ± 0.011°C and year-over-year with a maximum ret of 0.10 ± 0.01°C. In the current study, the temperature had raised by 0.5°C in 36 years, which fits well with the global rate of temperature change. There were differences in temperature changes among stations in the study area during the 36-years period 1980–2016.

The overall trends in average precipitation in the study area were increasing. Though the change was insignificant for this period, there was a change in precipitation for the last decade of this period that may affect the water supply system in the basin. Changes in average temperature and precipitation in the study area were observed during the 36-year (1980 to 2016) period, but the rates of change were different among stations in the study basin. It was observed that the mean annual average temperature increased while precipitation decreased in the whole basin during this period and climate change was found to have serious impacts in the study area (Figure 6). The result strongly supports our speculation climate change is one of the major driving forces that affects land cover change in the Abbay River Basin.

3.3.1. Analysis of Temperature. The ITA test shows an increasing trend in average condition. The trends of the average temperature for five stations are shown in Figure 7. The increasing trends of temperature were detected in Gondar station while decreasing trend was detected in Assosa station (Table 4).

The ITA results show that statistics are negative and positive values, most of them are significant. The ITA annual temperature shows an increasing trend in Assosa station ($\Phi = 2.63$), a statistically sharp decreasing trend in Bahir Dar station ($\Phi = -3.86$), a decreasing trend in Nedjo station ($\Phi = -1.78$), an increasing trend in Gondar station ($\Phi = 0.40$), in Motta station a statistically increasing trend was observed with ($\Phi = 0.30$), and finally a statistically significant increasing trend was observed in average condition (five stations) ($\Phi = 0.12$) (Table 5).

The MK trend annual temperature shows a decreasing trend in Assosa station ($Z = -2.61$), a statistically decreasing trend in Bahir Dar station ($Z = -2.63$), a statistically significant decreasing trend in Nedjo station ($Z = -3.53$), a significant increasing trend in Gondar station ($Z = 6.96$), a statistically significant increasing trend was observed in Motta station with ($Z = 4.58$), and, in general, a statistically significant increasing trend was observed in average condition (five stations) ($Z = 0.75$).

Annual temperature in the results of Sen's slope estimator test shows a sharply increasing trend observed in average condition ($Z = 0.75$). The ITA results (Figure 6) show that most points increase above the 1 : 1 line, an overall upward trend. However, the features of trends in annual mean temperature are quite distinct at each station. Figure 6 shows that the annual temperature significantly increased at the Gondar (Figure 7(c)) and Motta (Figure 7(e)), while at

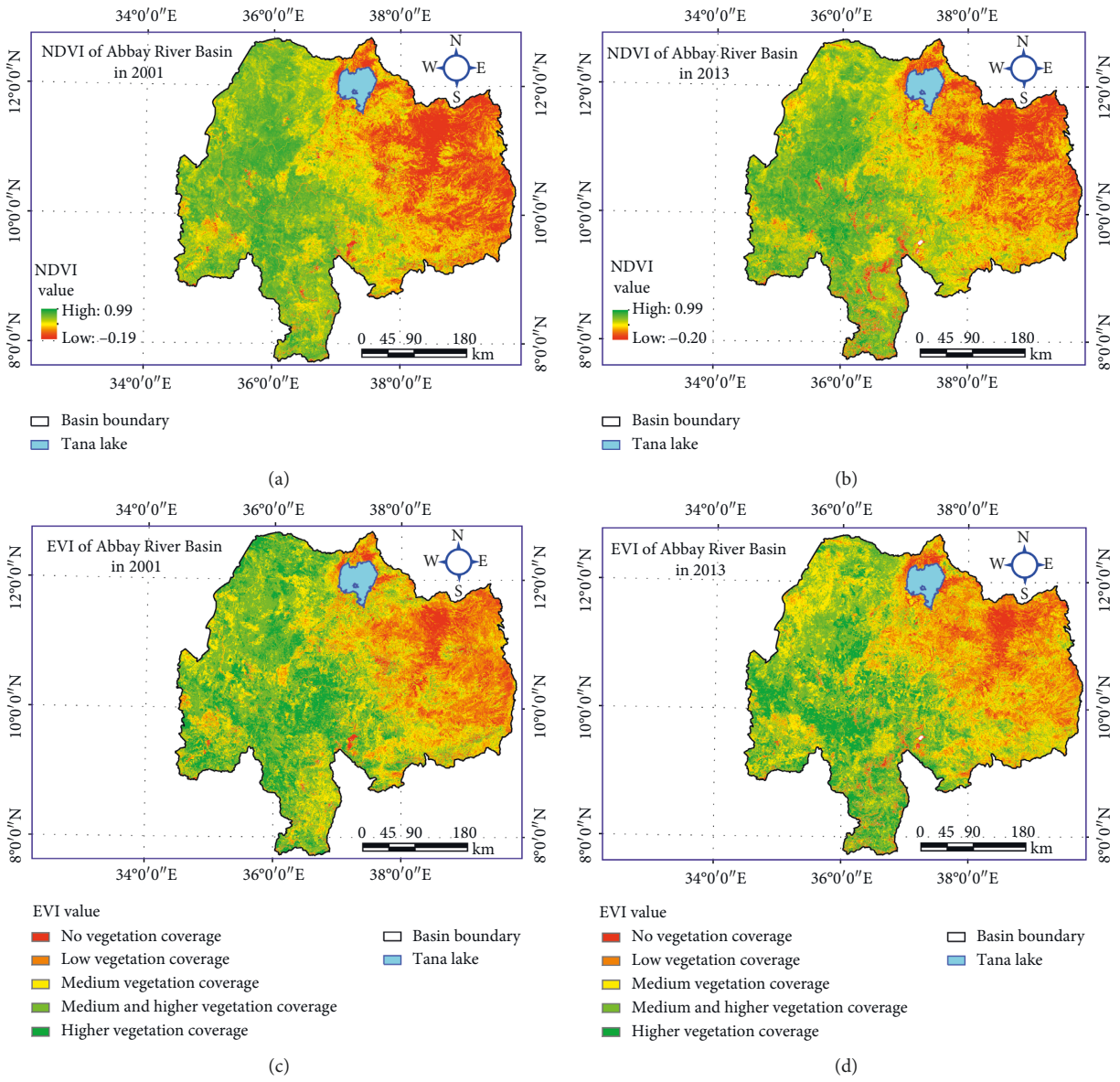

Figure 5: NDVI and EVA of Abbay River Basin in 2001 and 2013: (a) description of NDVI in 2001 and (b) description of NDVI in 2013; (c) description of EVI in 2001; and (d) description of EVI in 2013.

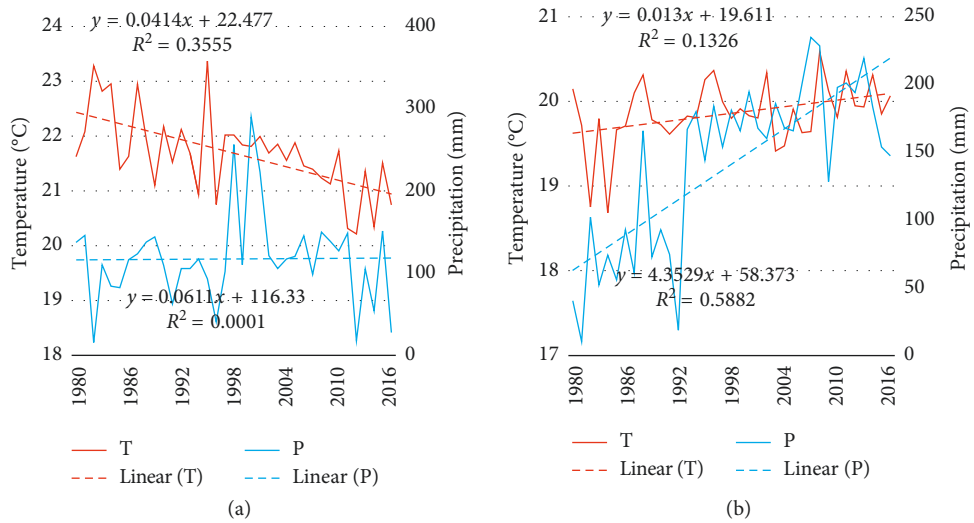

Figure 6: Continued.

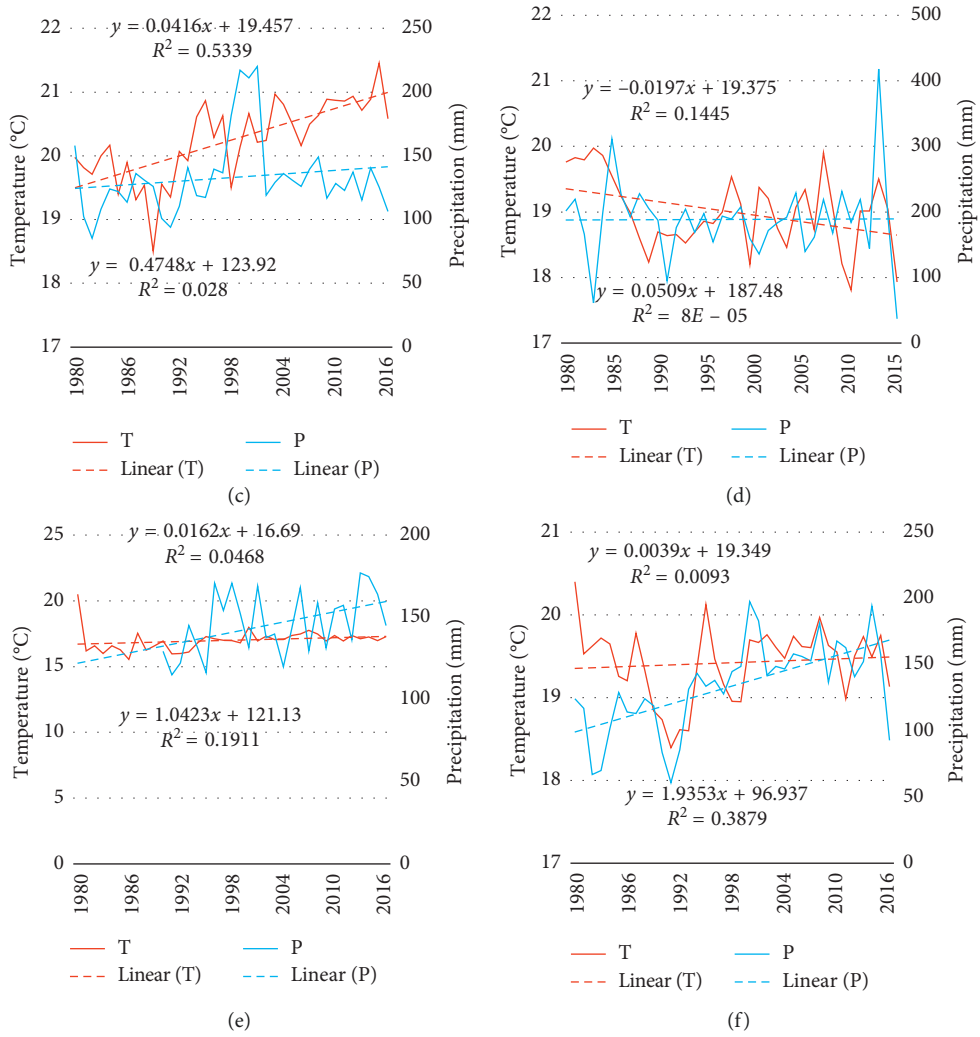

Figure 6: Description of the climate variability in Abbay River Basin. The temperature and precipitation trend for the period 1980–2016. The vertical column is temperature and horizontal column is precipitation change, and fluctuations line indicates annual values and breakdown lines indicate period running averages. (a) Asossa station. (b) Bahir Dar station. (c) Gondar station. (d) Nedjo station. (e) Motta station. (f) Average condition.

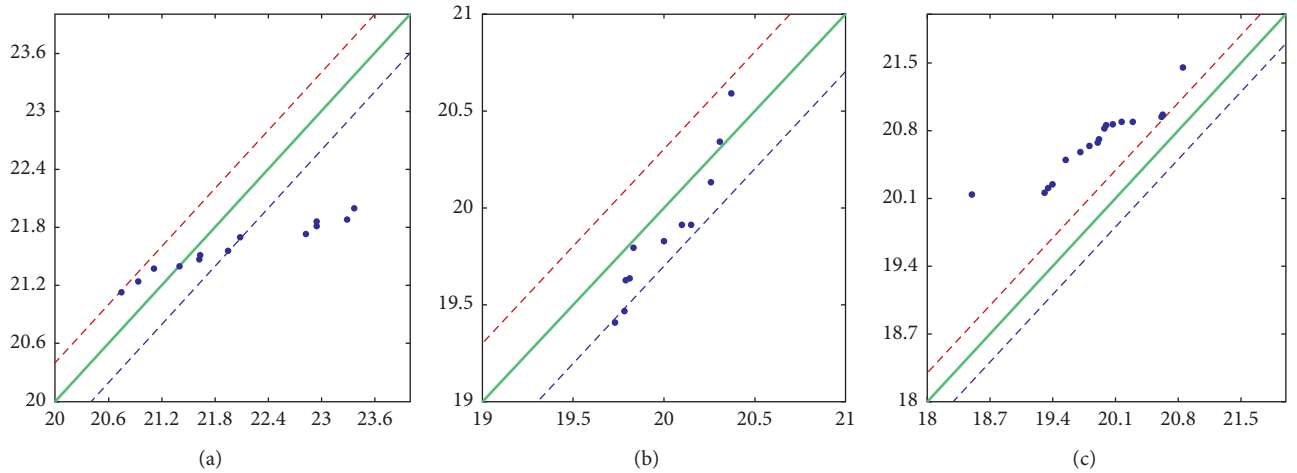

Figure 7: Continued.

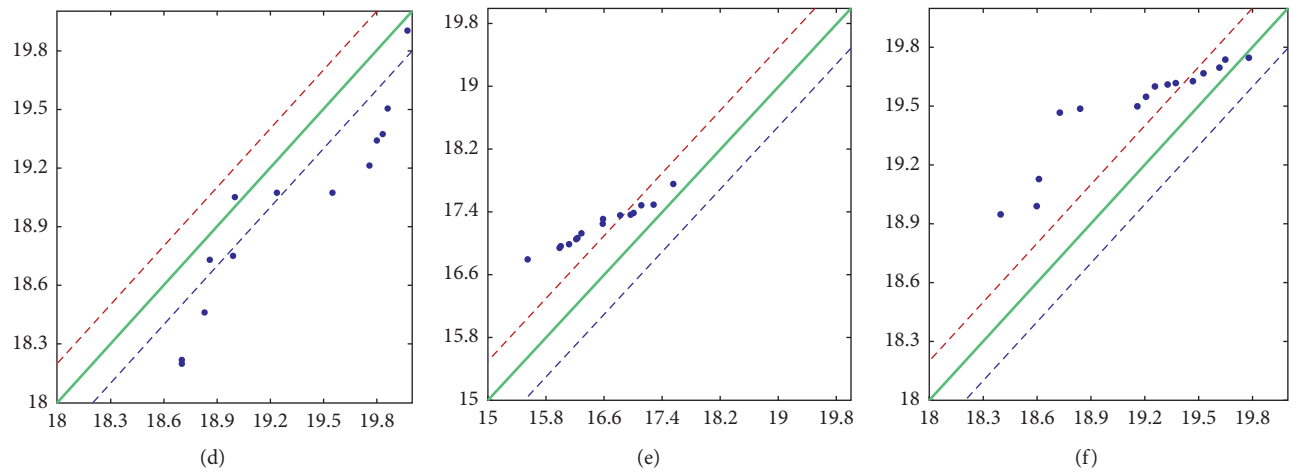

Figure 7: Results of ITA for annual temperature during 1986–2016. (a) Assosa station. (b) Bahir Dar station. (c) Gondar station. (d) Nedjo station. (e) Motta station. (f) Average condition.

Table 5: Trend test results of the annual average air temperature in the subbasins based on ITAM (Φ), MK (Z), and Sen's slope estimator test (β) analyses.

S/No.	Name of stations	Z (MK)	Φ	β
1	Assosa	-2.61^{**}	2.63^{**}	−0.03
2	Bahir Dar	-2.63^{**}	-3.86^{***}	−0.02
3	Nedjo	-3.53^{***}	-1.78^{*}	−0.03
4	Gondar	6.96^{***}	0.40	0.04
5	Motta	4.58^{***}	0.30	0.03
6	Average	0.75	0.12	0.00

*Trends at 0.1 significance level; **trends at 0.05 significance level; ***trends at 0.01 significance level.

the Assosa (Figure 7(a)), Bahir Dar (Figure 7(b)), and Nedjo (Figure 7(c)) stations, some points fall below the 1 : 1 line, some upward trend. But the trend of average annual temperature is increasing during 1978–2016 with respect to the 10% relative band.

3.3.2. Analysis of Precipitation. The trends of annual precipitation for five stations and average condition detected by the ITAM, MK, and Sen's slope estimator test are summarized in Table 6.

The ITA results showed that statistics are dominated by positive values, but most of them are insignificant. Five stations in average conditions were significant ($\Phi = 3.04$) A significant increasing trend was observed in Bahir Dar station ($\Phi = 28.91$) while the most decreasing trend was in the Nedjo station ($\Phi = 0.02$).

The MK results in annual precipitation showed a significant increasing trend in Motta station ($Z = 7.05$) while a significantly decreasing trend was observed in Nedjo station ($Z = -1.07$). A significant increasing trend was observed in average condition ($Z = 3.88$).

Sen's slope estimator test results of annual precipitation showed a significant increasing trend only in Bahir Dar station ($\beta = 5.71$) though other stations also showed positive values, with the exception of Nedjo station ($\beta = -0.46$) with a significant decreasing trend in Nedjo station ($\beta = -0.46$), and a significant increasing trend was observed in average condition ($\beta = 0.84$). The ITA results (Figure 8 and Table 6) show that the annual precipitation points fall between +10% to −10% lines, implying an overall downward trend at Nedjo station (Figure 8(d)), while it significantly increased at the Assosa (Figure 8(a)), Bahir Dar (Figure 8(b)), Gondar (Figure 8(c)), and Motta stations during 1986 to 2016 with respect to the 10% relative band (Figure 8).

3.4. Implication of Climate Change for Land Covers. As indicated in the previous sections of the paper, the temperature has increased by about 0.5°C during the period from 1980 to 2016 in the river basin. The biggest land cover change in the study area that has occurred is forest land cover, which had decreased pattern by 3429.62 km^2, and the water bodies were also decreased by 81.45 km^2. The changes were caused by climate variability, particularly increase in temperature as well as human activities in the region. Covers of cultivated land, grassland, bare land, wetland, and urban land in the study basin were increased from 2001 to 2013 as described above (Table 4). Water bodies were converted into wetland, forest land, and bare land by the area of 50.43 km^2, 11.75 km^2, and 21.30 km^2, respectively (Figure 4). The result of the study had indicated that land cover change is directly impacted by human activity. The vegetation covers in the river basin changed significantly in areas of intense human activities [43]. In the study area, deforestation had been taking place to some extent during the past decades, which was a major driving force for vegetation degradation. This consequently affects the climatic conditions of the study area. The effects of natural and human factors that affect land cover changes of the study area from 2001–2013 is described using a diagram shown in Figure 9.

4. Conclusions

In the study, the spatial and temporal land cover changes and vegetation evolution of the basin have been analyzed for the

Table 6: Trend test results of the mean precipitation in the subbasins based on ITAM (Φ), MK (Z), and Sen's slope estimator test (β) analysis.

S/No.	Name of stations	Z (MK)	Φ	β
1	Assosa	1.20*	5.87***	0.38
2	Bahir Dar	6.92***	28.91***	5.71***
3	Nedjo	−1.07*	0.02	−0.46***
4	Gondar	1.95*	1.88*	0.44
5	Motta	7.05***	14.82***	0.35
6	Average	3.88***	3.04***	0.84

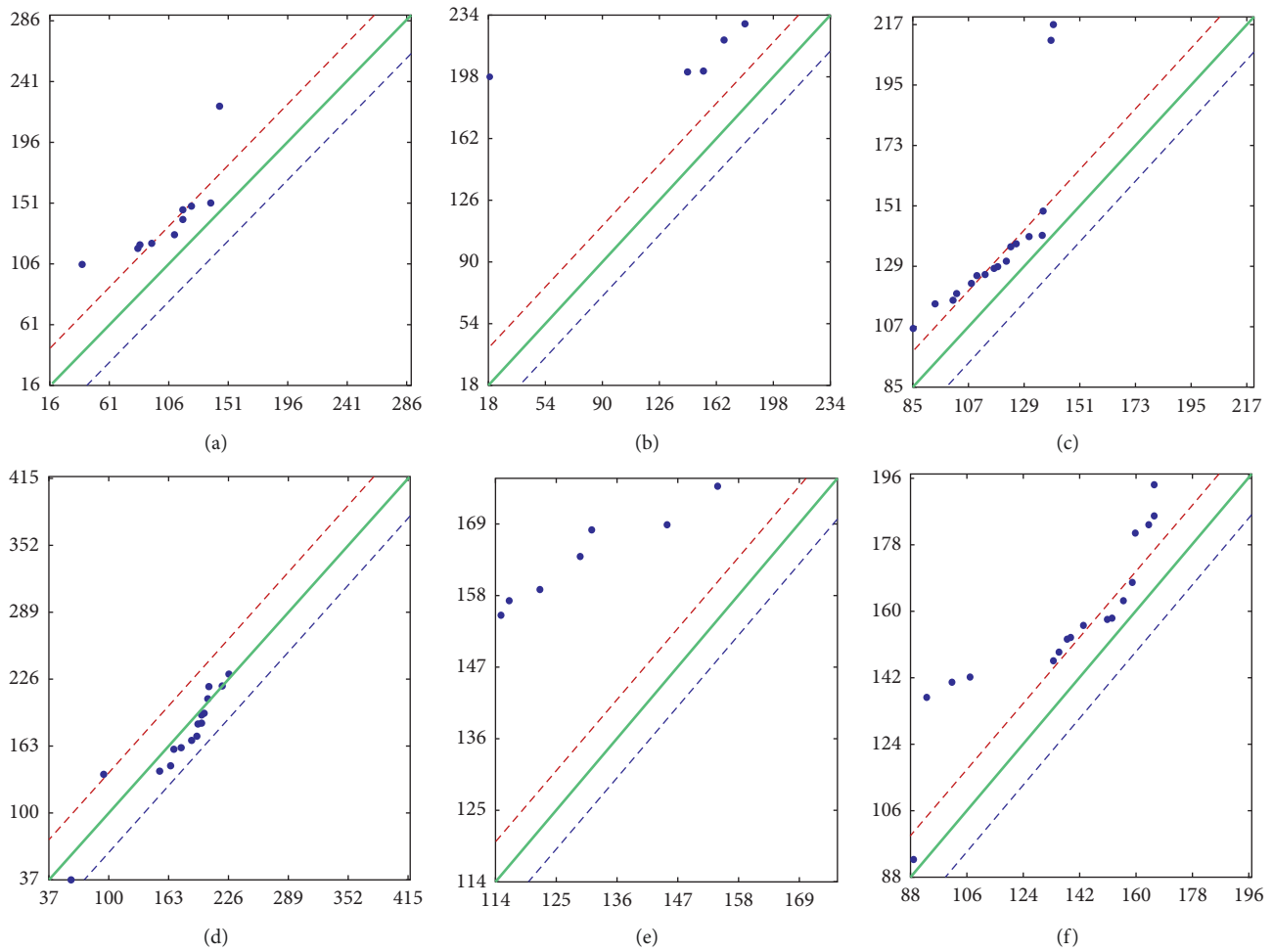

Figure 8: Results of ITA for annual precipitation during 1980–2016. (a) Assosa station. (b) Bahir Dar station. (c) Gondar station. (d) Nedjo station. (e) Motta station. (f) Average condition.

13-years period (2001 to 2013). The land cover changes that occurred in the study basin during the study period was deciphered using remote sensing, NDVI, EVI, and land classification methods and vegetation detection methods were employed to assess the change that comes in the study a period of 36 years (2001 to 2013). In the meantime, Mann–Kendall trend test, ITAM, and Sen's slope estimator test methods were used to analyze the variability of precipitation and temperature on annual basis in the study basin.

The result demonstrates that temperature has increased by 0.5°C while precipitation slightly changes in the river basin in a period spanning 1980 to 2016. The changes in climate change and particularly increment in air temperature was found as one of the driving forces for land cover change in the study area during this period. Analyses of the 13-years period (2001–2013) showed significant land cover changes in the study area. Land coverage of grassland, cultivated land, wetland, and urban and bare land showed a significant increase, whereas forest cover and water bodies decrease in the area. The changes in land cover were mainly caused by climate change and intense human socioeconomic activities in the region.

In the final analysis, land cover changes occurred in the Abbay River Basin during this time was statistically significant, and anthropogenic effects (human activity)

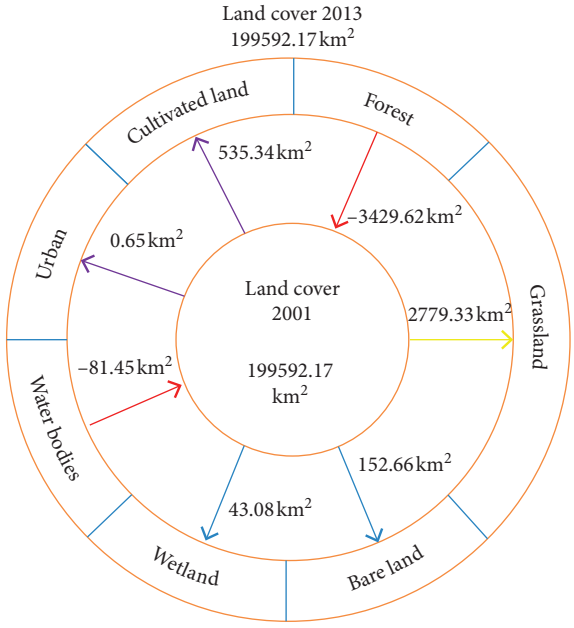

Figure 9: Diagram of natural, human, and climate impacts of land cover change of Abbey river basin in 2001–2013. Note: the arrows indicate a direction of gains and losses. The purple arrow indicates the impact of human activity which leads to the intensification of cultivation land and urbanization, the red arrow indicates the impact of the rise of temperature on the forest and water ecosystem, the yellow arrow indicates the impact of human and natural factor that has an influence on the natural ecosystem, and blue arrow indicates natural and other factors that have an impact on the ecosystem (Table 4).

and global and local climate were the major factors affecting, causing the shifts in land coverage profile. Thus, further research is warranted to study the potential influences of the land cover changes on hydro-ecological processes in the river basin that will have important implications to design sustainable development policies in the river basin.

Data Availability

The data used to support the findings of this study are available from the first author upon request.

Conflicts of Interest

The authors declare no conflicts of interest.

Authors' Contributions

A. A. and Y. D. were responsible for conceptualization; H. W. was involved in methodology; D. B., O. Y., and H. W. were responsible for software; A. G., M. G., and T. Q. were involved in validation; M. T. K. performed formal analysis; T. Q. investigated the study; A. G. was responsible for resources; M. G. was responsible for data source; A. A. wrote, reviewed, and edited the original draft; A. G. and D. B. were involved in visualization; Y. D. and X. S. supervised the study; H. W. was involved in project administration; T. Q. was responsible for funding acquisition.

Acknowledgments

The authors would like to thank the China Institute of Water Resources and Hydropower Research for financing this research and Donghua University. This research was funded by the National Key Research and Development Project (Grant no. 2016YFA0601503), China.

References

[1] J. Feng, D. Yan, C. Li, F. Yu, and C. Zhang, "Assessing the impact of climatic factors on potential evapotranspiration in droughts in North China," *Quaternary International*, vol. 336, pp. 6–12, 2014.

[2] D. Conway, "A water balance model of the upper blue Nile in Ethiopia," *Hydrological Sciences Journal*, vol. 42, no. 2, pp. 265–286, 1997.

[3] D. N. Yates and K. M. Strzepek, "Modeling the Nile basin under climatic change," *Journal of Hydrologic Engineering*, vol. 3, no. 2, pp. 98–108, 1998.

[4] R. A. Wurbs, R. S. Muttiah, and F. Felden, "Incorporation of climate change in water availability modeling," *Journal of Hydrologic Engineering*, vol. 10, no. 5, pp. 375–385, 2005.

[5] J. J. Lawler, D. J. Lewis, E. Nelson et al., "Projected land-use change impacts on ecosystem services in the United States," *Proceedings of the National Academy of Sciences*, vol. 111, no. 20, pp. 7492–7497, 2014.

[6] S. G. Gebrehiwot, W. Bewket, A. I. Gärdenäs, and K. Bishop, "Forest cover change over four decades in the blue Nile basin, Ethiopia: comparison of three watersheds," *Regional Environmental Change*, vol. 14, no. 1, pp. 253–266, 2014.

[7] D. E. Pozen, "The mosaic theory, national security, and the freedom of information act," *The Yale Yellow Journal*, vol. 155, 2005.

[8] M. Bekele, "Forest property rights, the role of the state, and intitutional exigency the Ethiopian experience," Doctoral thesis, Swedish University of Agricultural Science, Uppsala, Sweden, 2003.

[9] R. S. DeFries, T. Rudel, M. Uriarte, and M. Hansen, "Deforestation driven by urban population growth and agricultural trade in the twenty-first century," *Nature Geoscience*, vol. 3, no. 3, pp. 178–181, 2010.

[10] G. Li, F. Zhang, Y. Jing, Y. Liu, and G. Sun, "Response of evapotranspiration to changes in land use and land cover and climate in China during 2001–2013," *Science of The Total Environment*, vol. 596-597, pp. 256–265, 2017.

[11] E. Haile and M. Assefa, "The impact of land use change on the hydrology of the Angereb watershed, Ethiopia," *International Journal of Water Sciences*, vol. 1, p. 1, 2012.

[12] G. T. Eshete, "Biodiversity and livelihoods in southwestern Ethiopia: forest loss and prospects for conservation in shade coffee agroecosystems," UC Santa Cruz, Santa Cruz, CA, USA, Doctoral dissertation, 2013.

[13] N. Haregeweyn, A. Tsunekawa, M. Tsubo et al., "Analyzing the hydrologic effects of region-wide land and water development interventions: a case study of the upper blue Nile basin," *Regional Environmental Change*, vol. 16, no. 4, pp. 951–966, 2016.

[14] M. K. Emily Schmidt, "Urbanization and spatial connectivity in Ethiopia: urban growth analysis using GIS," International

Food Policy Research Institute, Washington, DC, USA, ESSP2 Discussion Paper 003, 2009.

[15] J. Kearney, "Food consumption trends and drivers," *Philosophical Transactions of the Royal Society B: Biological Sciences*, vol. 365, no. 1554, pp. 2793–2807, 2010.

[16] M. Blumstein and J. R. Thompson, "Land-use impacts on the quantity and configuration of ecosystem service provisioning in Massachusetts, USA," *Journal of Applied Ecology*, vol. 52, no. 4, pp. 1009–1019, 2015.

[17] A. D. Yilma and S. B. Awulachew, "Characterization and atlas of the blue Nile basin and its sub basins," *Atlas*, 2009.

[18] S. Tekleab, Y. Mohamed, and S. Uhlenbrook, "Hydro-climatic trends in the abay/upper blue Nile basin, Ethiopia," *Physics and Chemistry of the Earth, Parts A/B/C*, vol. 61-62, pp. 32–42, 2013.

[19] U. Kim and J. J. Kaluarachchi, "Climate change impacts on water resources in the upper blue Nile river basin, Ethiopia1," *JAWRA Journal of the American Water Resources Association*, vol. 45, no. 6, pp. 1361–1378, 2009.

[20] T. Abate and A. Angassa, "Conversion of savanna rangelands to bush dominated landscape in Borana, Southern Ethiopia," *Ecological Processes*, vol. 5, no. 1, p. 6, 2016.

[21] B. Dorjsuren, D. Yan, H. Wang et al., "Observed trends of climate and land cover changes in Lake Baikal basin," *Environmental Earth Sciences*, vol. 77, no. 20, p. 725, 2018.

[22] M. Gebreyes, "Assessing the effectiveness of planned adaptation interventions in reducing local level vulnerability. Adapting to climate change in the water sector," Working Paper 18, 2010.

[23] A. O. Owojori, "Landsat image-based lulc changes of San Antonio, Texas using advanced atmospheric correction and object-oriented image analysis approaches," *Remote Sensing Image Processing and Analysis (ES 6973)*, 2005.

[24] A. Butt, R. Shabbir, S. S. Ahmad, and N. Aziz, "Land use change mapping and analysis using remote sensing and GIS: a case study of simly watershed, Islamabad, Pakistan," *The Egyptian Journal of Remote Sensing and Space Science*, vol. 18, no. 2, pp. 251–259, 2015.

[25] R. Manandhar, I. O. A. Odeh, and T. Ancev, "Improving the accuracy of land use and land cover classification of Landsat data using post-classification enhancement," *Remote Sensing*, vol. 1, no. 3, pp. 330–344, 2009.

[26] K. Gwet, "Kappa statistic is not satisfactory for assessing the extent of agreement between raters," *Statistical Methods For Inter-Rater Reliability Assessment*, no. 1, 2002.

[27] S. N. Goward, B. Markham, D. G. Dye, W. Dulaney, and J. Yang, "Normalized difference vegetation index measurements from the advanced very high resolution radiometer," *Remote Sensing of Environment*, vol. 35, no. 2-3, pp. 257–277, 1991.

[28] S. Yue and C. Wang, "The Mann-Kendall test modified by effective sample size to detect trend in serially correlated hydrological series," *Water Resources Management*, vol. 18, no. 3, pp. 201–218, 2004.

[29] J. W. Rouse, H. R. Haas, J. A. Scheel, and D. W. Deering, "Monitoring vegetation systems in the great plains with ERTS NASA," in *Proceedings of the Goddard Space Flight Center 3d ERTS-1 Symposium*, vol. 1, pp. 309–317, Washington, DC, USA, January 1974.

[30] Z. Şen, "Trend identification simulation and application," *Journal of Hydrologic Engineering*, vol. 19, no. 3, pp. 635–642, 2014.

[31] L. Cui, L. Wang, Z. Lai, Q. Tian, W. Liu, and J. Li, "Innovative trend analysis of annual and seasonal air temperature and rainfall in the Yangtze river basin, China during 1960–2015," *Journal of Atmospheric and Solar-Terrestrial Physics*, vol. 164, pp. 48–59, 2017.

[32] O. Kisi, "An innovative method for trend analysis of monthly pan evaporations," *Journal of Hydrology*, vol. 527, pp. 1123–1129, 2015.

[33] Z. Şen, "Innovative trend analysis methodology," *Journal of Hydrologic Engineering*, vol. 17, no. 9, pp. 1042–1046, 2012.

[34] B. Dorjsuren, D. Yan, H. Wang et al., "Observed trends of climate and river discharge in Mongolia's Selenga sub-basin of the lake Baikal basin," *Water*, vol. 10, no. 10, p. 1436, 2018.

[35] H. B. Mann, "Nonparametric tests against trend," *Econometrica*, vol. 13, no. 3, pp. 245–259, 1945.

[36] M. Gedefaw, H. Wang, D. Yan et al., "Trend analysis of climatic and hydrological variables in the Awash river basin, Ethiopia," *Water*, vol. 10, no. 11, p. 1554, 2018.

[37] M. Gedefaw, D. Yan, H. Wang et al., "Innovative trend analysis of annual and seasonal rainfall variability in Amhara regional state, Ethiopia," *Atmosphere*, vol. 9, no. 9, p. 326, 2018.

[38] Atta-ur-Rahman and M. Dawood, "Spatio-statistical analysis of temperature fluctuation using Mann–Kendall and Sen's slope approach," *Climate Dynamics*, vol. 48, no. 3-4, pp. 783–797, 2017.

[39] A. A. Akinsanola and K. O. Ogunjobi, "Recent homogeneity analysis and long-term spatio-temporal rainfall trends in Nigeria," *Theoretical and Applied Climatology*, vol. 128, no. 1-2, pp. 275–289, 2017.

[40] F. Liu, T. Qin, A. Girma et al., "Dynamics of land-use and vegetation change using NDVI and transfer matrix: a case study of the Huaihe river basin," *Polish Journal of Environmental Studies*, vol. 28, no. 1, pp. 213–223, 2018.

[41] Y. Arsano and I. Tamrat, "Ethiopia and the Eastern Nile basin," *Aquatic Sciences*, vol. 67, no. 1, pp. 15–27, 2005.

[42] V. S. Seleshi Bekele Awulachew and D. P. David Molden, *The Nile River Basin Water, Agriculture, Governance And Livelihoods*, Routledge, New York, NY, USA, 2012.

[43] D. H. Yan, H. Wang, H. H. Li et al., "Quantitative analysis on the environmental impact of large-scale water transfer project on water resource area in a changing environment," *Hydrology and Earth System Sciences*, vol. 16, no. 8, pp. 2685–2702, 2012.